

On the dust and gas content of high-redshift galaxies hosting obscured AGN in the CDF-S

Quirino D'Amato

INAF - Istituto di Radioastronomia
Alma Mater Studiorum – Università di Bologna

C.Vignali, R. Gilli, M. Massardi, C. Circosta

ALMA Science and Proposals Workshop – February 27th 2019

Obscured AGN

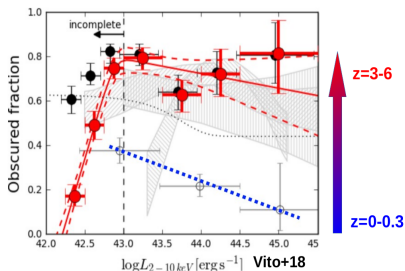
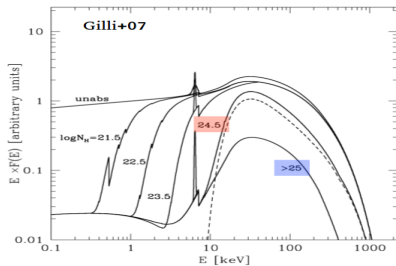
Outline

Scientific rationale and targets

Data analysis

Results

Conclusions and future perspectives



- **Unabsorbed:**
 $\log N_H < 21$
- **Compton thin:**
 $21 < \log N_H < 24$
- **Mildly Compton thick:**
 $\log N_H \sim 24 - 25$
- **Heavily Compton thick:**
 $\log N_H > 25$

obscured AGN fraction increases at high redshift

Sub-Millimetre Galaxies

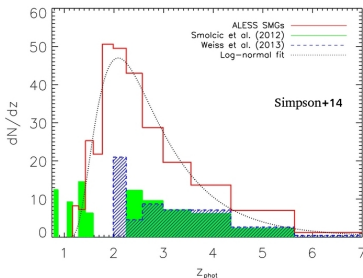
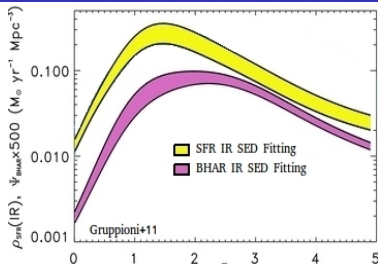
Outline

Scientific rationale and targets

Data analysis

Results

Conclusions and future perspectives



SFR density and BH accretion density peak at $z \approx 2$

SMGs

- Peak at $z \approx 2$
- $M_{*} \sim 10^{10-11} M_{\odot}$
- $M_d \sim 10^8 M_{\odot}$
- $M_{H_2} \sim 10^{10} M_{\odot}$
- $\text{SFR} \sim 10^{2-3} M_{\odot}/\text{yr}$
- $\tau_d \sim 10^8 \text{ yr}$
- AGN fraction:
 - ~ 0.5 ($L_{\text{IR}} < 10^{12} L_{\odot}$)
 - ~ 0.9 ($L_{\text{IR}} > 10^{12} L_{\odot}$)
- Size \sim few kpc

Contribution of the host galaxy to the AGN obscuration?

Objectives and targets

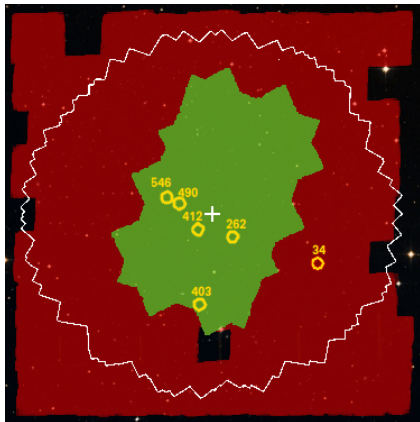
Outline

Scientific rationale and targets

Data analysis

Results

Conclusions and future perspectives



White contour: CDF-S
Red area: GEMS
Green area: CANDELS
28' × 28'

Parent samples

- 34 AGN at $z > 3$, selected in the 4-Ms CDF-S (Vito+13)
- 8 AGN at $z = 1.1-3.7$, selected in the 1-Ms CDF-S (Rigopoulou+09)

Selection criteria

- Secure spectroscopic $z > 2.5$
- Column density $\log N_H > 23$
- Detection at $\lambda_{obs} > 100\mu\text{m}$

Derived sample: 6 sources

- $2.5 < z < 4.7$
- 260–2000 counts in the 7-Ms CDF-S,
($2 < L_{2-10\text{keV}} < 6$) $\times 10^{44}$ erg s $^{-1}$
- $\text{SFR} \sim 10^{2-3} M_{\odot}/\text{yr}$
- $M_* \sim 10^{11} M_{\odot}$

Moments of the line

Outline

Scientific rationale and targets

Data analysis

Results

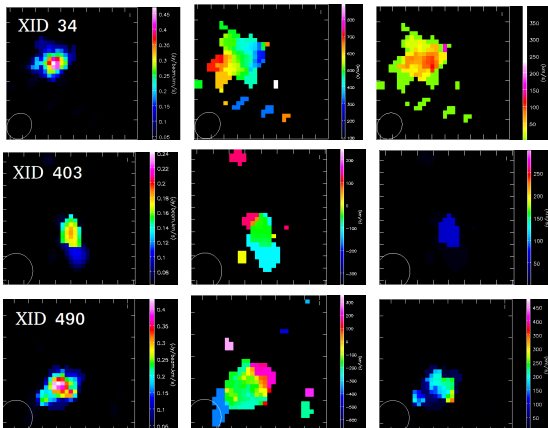
Conclusions and future perspectives

Three sources detected in continuum and CO

Flux

Velocity map

Velocity dispersion



- XID 34: Chaotic structure
- XID 403,490: Rotating features
- Beam size: Poor resolution

Considered channels:
 $v_0 \pm FWHM$

Image pixels $> 3\sigma$
Image sizes $\sim 2.7''$

Spectral fitting

Outline

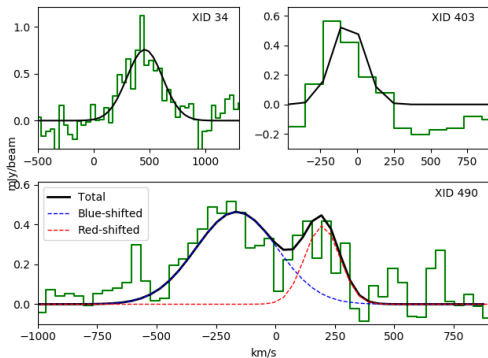
Scientific rationale and targets

Data analysis

Results

Conclusions and future perspectives

Gaussian fitting of the lines



| XID | v_0 (km/s) | FWHM (km/s) |
|--------------|-----------------|----------------|
| 34 | 498 ± 14 | 368 ± 32 |
| 403 | -56 ± 33 | 308 ± 77 |
| 490(Blue c.) | -194 ± 26 | 474 ± 67 |
| 490(Red c.) | 187 ± 12 | 162 ± 27 |

XID 34: the velocity peak is ~ 500 km/s shifted wrt the rest-frame velocity at the spectroscopic redshift

XID 490: double-peaked line, likely Doppler effect

XID 34: Merger?

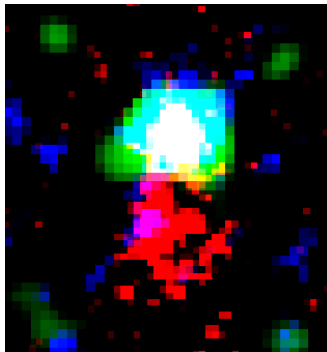
Outline

Scientific rationale and targets

Data analysis

Results

Conclusions and future perspectives



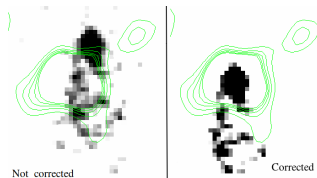
Red: V-band (~ 600 nm) HST

Green: ALMA continuum $\text{@}3\sigma$

Blue: ALMA CO $\text{@}3\sigma$

Image size: 0.6×0.9 arcsec

Relative motion between gas and SF component



Watchout for astrometry!

Fitting model: 2-D Gaussian in the visibilities space

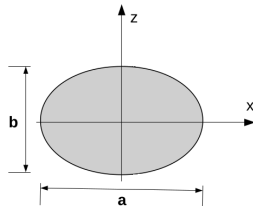
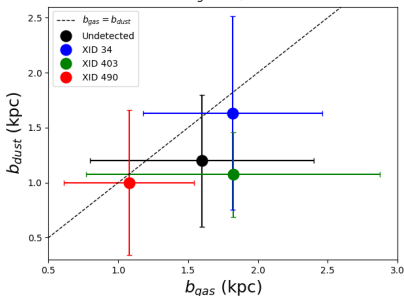
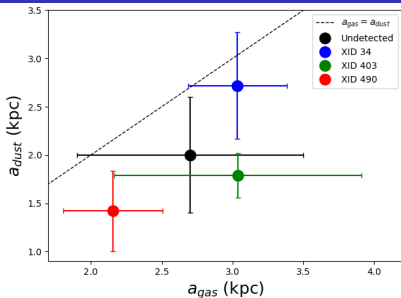
Outline

Scientific rationale and targets

Data analysis

Results

Conclusions and future perspectives



Assumptions

- **Undetected sources:** Size = mean of the detected sources, Error on a = 30%, Error on b = 50%
- **XID 490 dust b :** XID 490 dust b : Unconstrained by the fitting, assuming $R = 0.8$ (from the non-deconvolved image fitting), Error on R = 50%

Size gas > Size dust

Gas mass - Different approaches

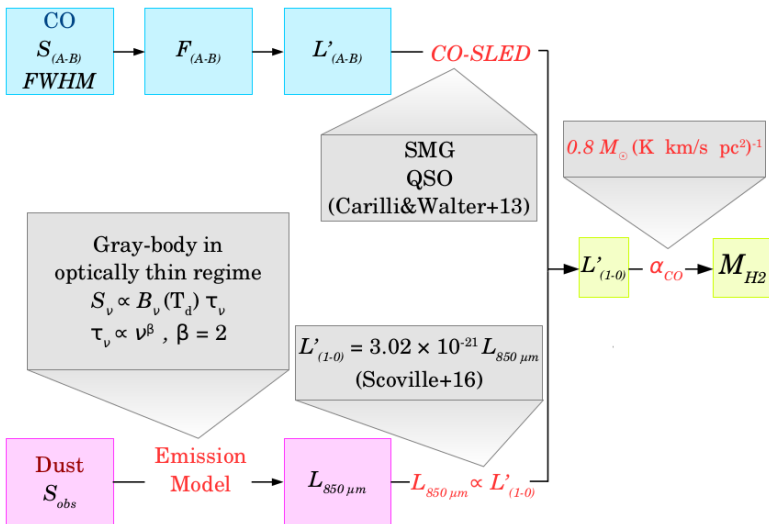
Outline

Scientific rationale and targets

Data analysis

Results

Conclusions and future perspectives



Gas mass

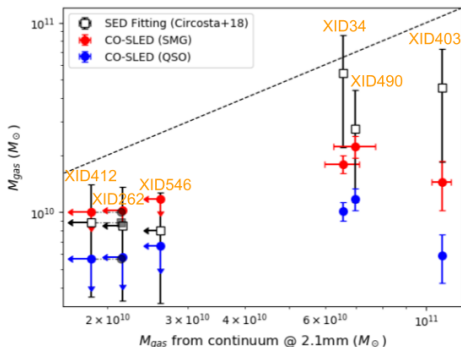
Outline

Scientific rationale and targets

Data analysis

Results

Conclusions and future perspectives



$$M_{H_2}^{DUST} > M_{H_2}^{CO-SLED}$$

$$M_{H_2}^{SMG} > M_{H_2}^{QSO}$$

Undetected sources

Upper limits at the 3σ level measured on the images for both the line and continuum emissions.

Column density – Uniform sphere

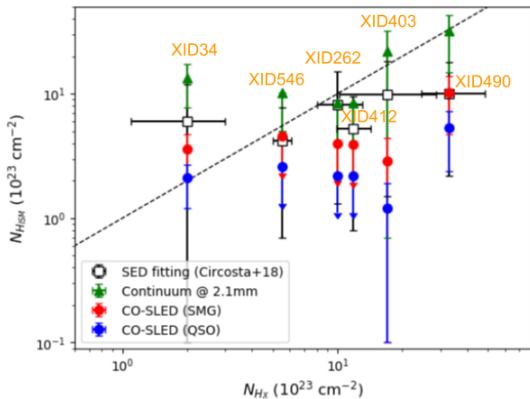
Outline

Scientific rationale and targets

Data analysis

Results

Conclusions and future perspectives



Notes

- N_{Hx} from X-ray spectral fitting
- Upper limits at the 3σ level

N_{Hx} and N_{HISM} :
same order of
magnitude

Host ISM can
significantly contribute
to the obscuration of
the central AGN

Column density – Rotating “coin” disk

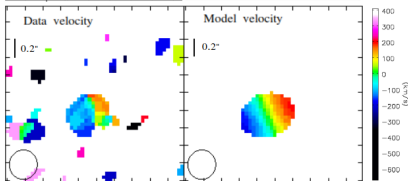
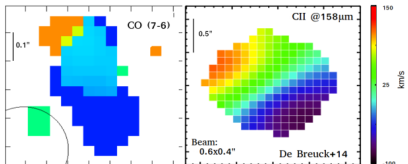
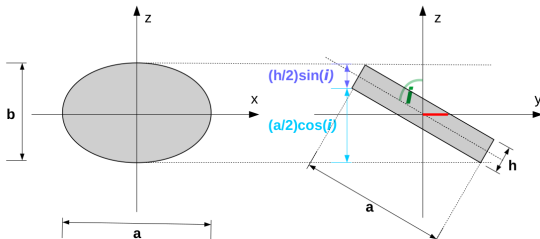
Outline

Scientific rationale and targets

Data analysis

Results

Conclusions and future perspectives



$$b_G = a_G \cos(i) + h_G \sin(i)$$

$$\text{XID 403: } i = 53^\circ$$

$$\text{XID 490: } i = 40.5^\circ$$

$$N_{HISM}^{disk} \approx 10 N_{HISM}^{sphere}$$

**POORLY
CONSTRAINED**

Dust mass and temperature

Outline

Scientific rationale and targets

Data analysis

Results

Conclusions and future perspectives

| XID | T (K) | M_d ($10^8 M_\odot$) |
|-----|-------|--------------------------|
| 262 | 71 | < 1.0 |
| 412 | 80 | < 0.9 |
| 34 | 55 | 4.9 ± 0.7 |
| 403 | 65 | 4.8 ± 0.5 |
| 546 | 65 | < 1.5 |
| 490 | 69 | 4.2 ± 0.5 |

Temperature

Single temperature (error $\approx \pm 5$ K), gray body IR-SED fitting:

$$S_\nu \propto B_\nu(T_d)\tau$$

$$\tau \propto \nu^\beta, \beta = 2$$

Mass

$$M_d = \frac{D_L^2 S_{obs}}{k_\nu B_\nu(T_d)(1+z)}$$

$$k_\nu \propto \nu^\beta, \beta = 2$$

Dynamical mass

Outline

Scientific rationale and targets

Data analysis

Results

Conclusions and future perspectives

$$M_{dyn} \sin^2 i = 6.5 \cdot 10^4 \left(\frac{FWHM}{\text{km s}^{-1}} \right)^2 \left(\frac{a}{\text{kpc}} \right) M_{\odot} \text{ (Wang+13, Calura+14)}$$

Assuming $v_{c,max} = 0.75FWHM$

$$\text{XID 403: } M_{dyn} \sin^2 i = 1.8_{-0.9}^{+1.7} \times 10^{10} M_{\odot} \text{ (Coppin+10, De Breuk+14)}$$

$$\text{XID 490: } M_{dyn} \sin^2 i = 1.4_{-0.3}^{+0.3} \times 10^{10} M_{\odot}$$

$$M_{bar} = M_{*} + M_{H_2} + M_{HI} \approx 10^{11} M_{\odot}, \sim 10 M_{dyn} \sin^2 i$$

M_{*} from SED fitting, $M_{HI} \sim M_{H_2}/5$ (Calura+14)

For $M_{dyn} \approx M_{bar} \rightarrow |i| \lesssim 10^{\circ}$, $h \gtrsim 6$ kpc **UNREALISTIC**

Possible causes

- Underestimate $M_{dyn} \sin^2 i$ conversion factor
- Different CANDELS/HST emitting region size wrt ALMA
- Uncertainty on position of $v_{c,max}$, underestimate a due to low sensitivity

Conclusions and future perspectives

Outline

Scientific rationale and targets

Data analysis

Results

Conclusions and future perspectives

- Sources have $M_{H_2} \sim 10^{10} M_{\odot}$ and $M_d \sim 10^8 M_{\odot}$ confined in few kpc scale.
 - The host galaxy ISM can significantly contribute to the obscuration of the central AGN for both spherical and disk model. N_{HISM}^{SMG} is more consistent with N_{H_X} than N_{HISM}^{QSO} .
 - Rotating systems and one possible merger.
-
- Future observations at better resolution ($< 0.1''$) and higher sensitivity (~ 6 h exposure to halve the current sensitivity) would drastically reduce the uncertainties on the physical quantities derived in this work.
 - XID 403: CO-SLED coupling measured CO(7-6) with CO(2-1) by Coppin+2010 and CO(12-11) by Nagao+12 (upper limit).

Outline

Scientific
rationale and
targets

Data analysis

Results

Conclusions
and future
perspectives

*THANKS
FOR YOUR
ATTENTION!*



Continuum images

Outline

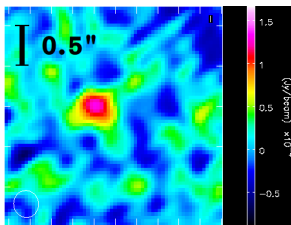
Scientific rationale and targets

Data analysis

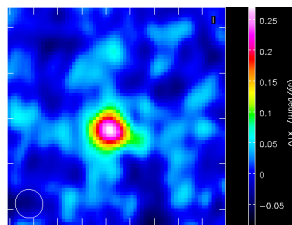
Results

Conclusions and future perspectives

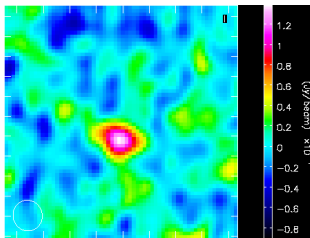
XID 34



XID 403



XID 490



Data fitting – Procedure

Outline

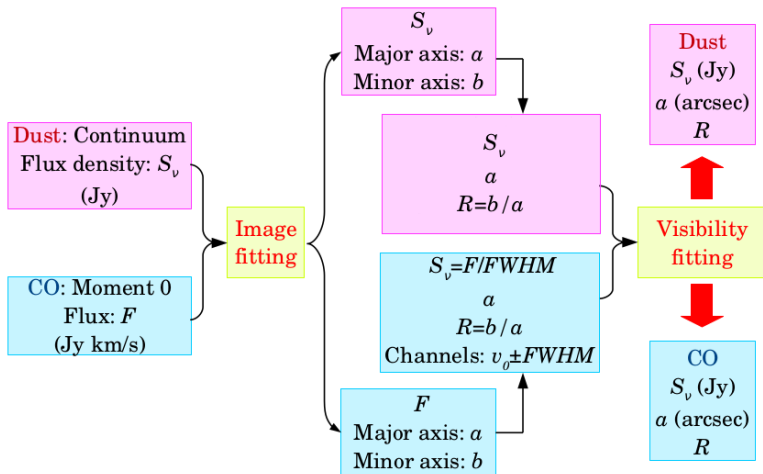
Scientific rationale and targets

Data analysis

Results

Conclusions and future perspectives

Fitting model: 2-D Gaussian



Fitting Results

Outline

Scientific rationale and targets

Data analysis

Results

Conclusions and future perspectives

CO line

| XID | Flux density (mJy) | Major axis (arcsec) | Axial ratio |
|-----|-----------------------|------------------------|---------------|
| 34 | 1.5 ± 0.1 | 0.38 ± 0.04 | 0.6 ± 0.2 |
| 403 | 0.7 ± 0.1 | 0.46 ± 0.13 | 0.6 ± 0.3 |
| 490 | 1.01 ± 0.07 | 0.26 ± 0.04 | 0.5 ± 0.2 |

Dust Continuum

| XID | Flux density (mJy) | Major axis (arcsec) | axial ratio |
|-----|-----------------------|------------------------|---------------|
| 34 | 0.23 ± 0.02 | 0.34 ± 0.07 | 0.6 ± 0.3 |
| 403 | 0.41 ± 0.02 | 0.27 ± 0.03 | 0.6 ± 0.2 |
| 490 | 0.19 ± 0.02 | 0.17 ± 0.05 | - |

Geometrical models – Rotating disk

Outline

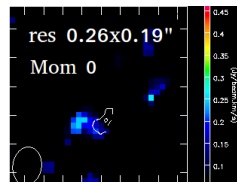
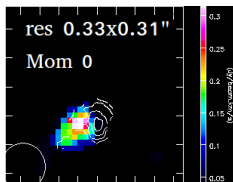
Scientific rationale and targets

Data analysis

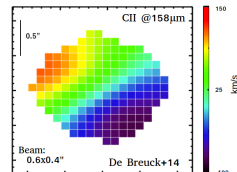
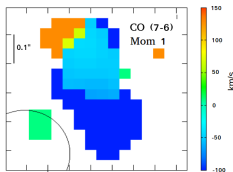
Results

Conclusions and future perspectives

XID 490
Double peak,
velocity maps



XID 403



Displacement

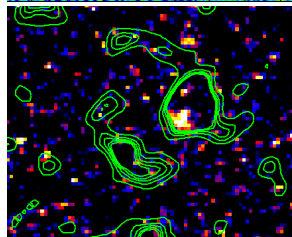
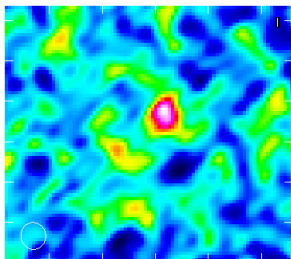
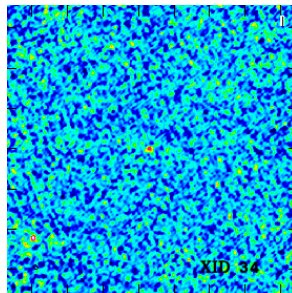
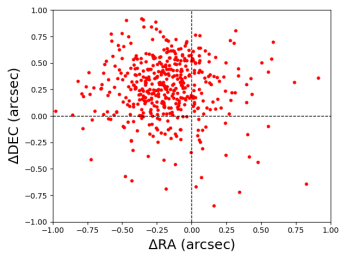
Outline

Scientific rationale and targets

Data analysis

Results

Conclusions and future perspectives



CO-SLEDs and Scoville relation

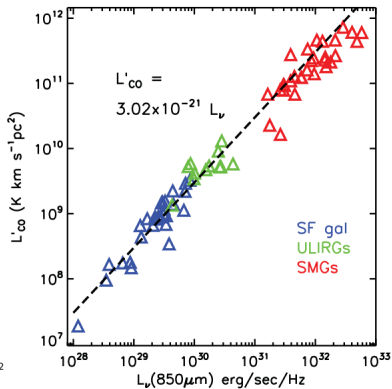
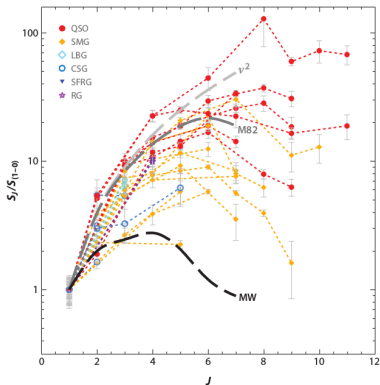
Outline

Scientific rationale and targets

Data analysis

Results

Conclusions and future perspectives



XID 490 – X-ray spectral fitting

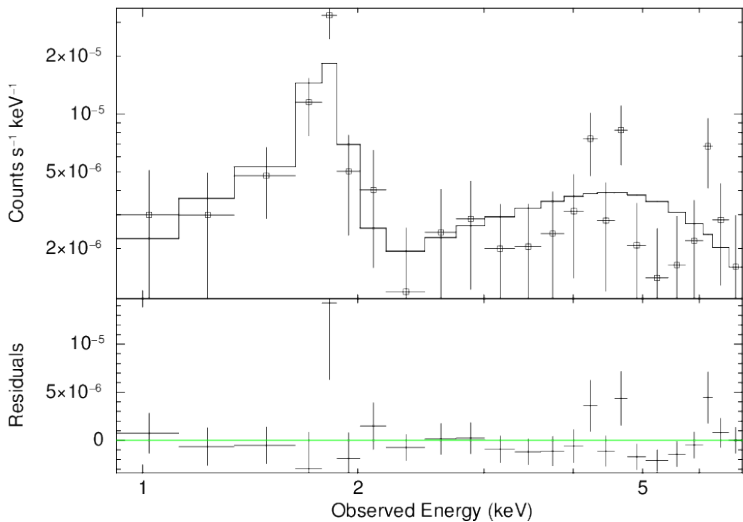
Outline

Scientific rationale and targets

Data analysis

Results

Conclusions and future perspectives



XID 490 – IR SED

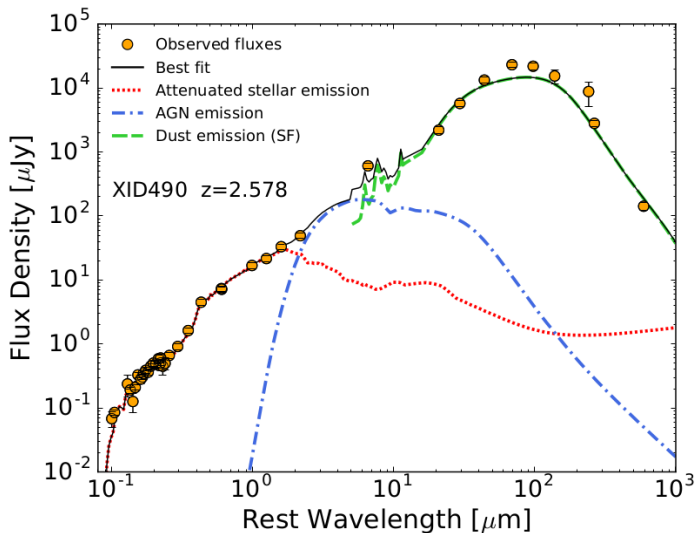
Outline

Scientific rationale and targets

Data analysis

Results

Conclusions and future perspectives



XID 490 – optical spectrum

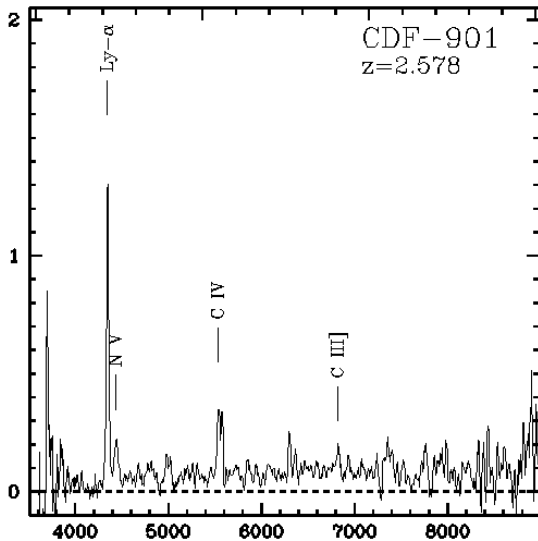
Outline

Scientific rationale and targets

Data analysis

Results

Conclusions and future perspectives



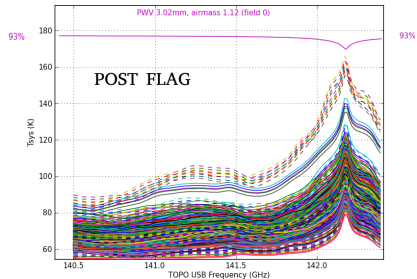
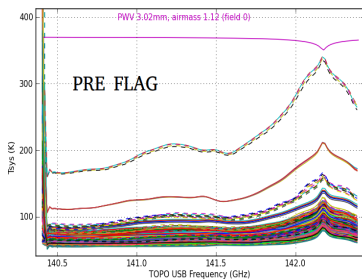
Outline

Scientific
rationale and
targets

Data analysis

Results

Conclusions
and future
perspectives



UV distance

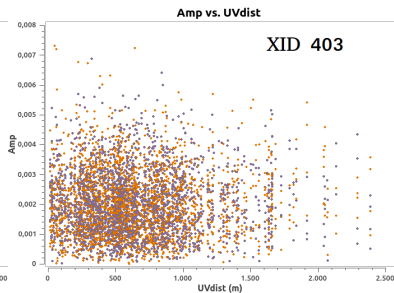
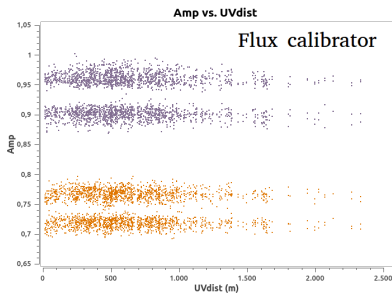
Outline

Scientific
rationale and
targets

Data analysis

Results

Conclusions
and future
perspectives



Phase and bandpass calibration

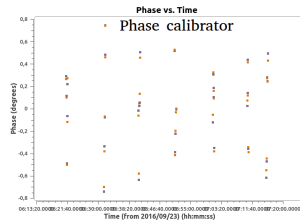
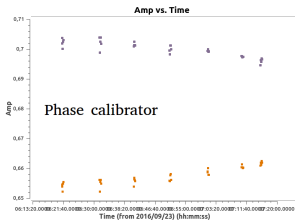
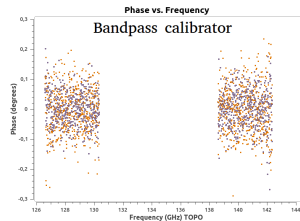
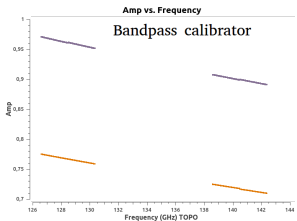
Outline

Scientific rationale and targets

Data analysis

Results

Conclusions and future perspectives



CO peak channels

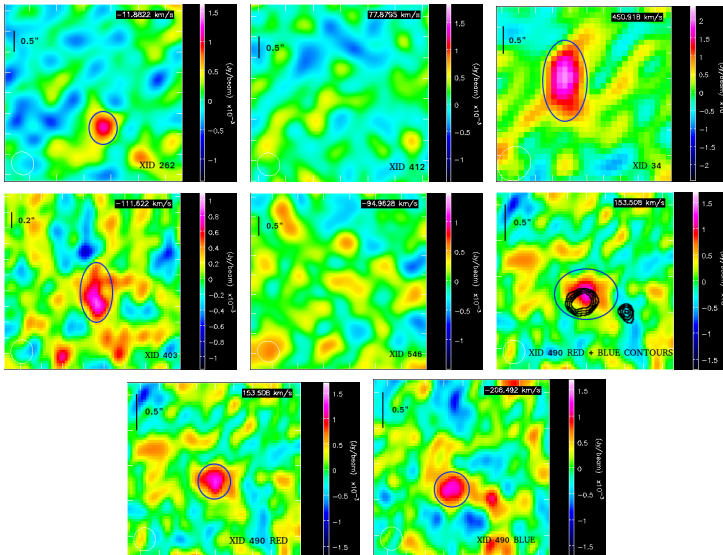
Outline

Scientific rationale and targets

Data analysis

Results

Conclusions and future perspectives



Total Spectra

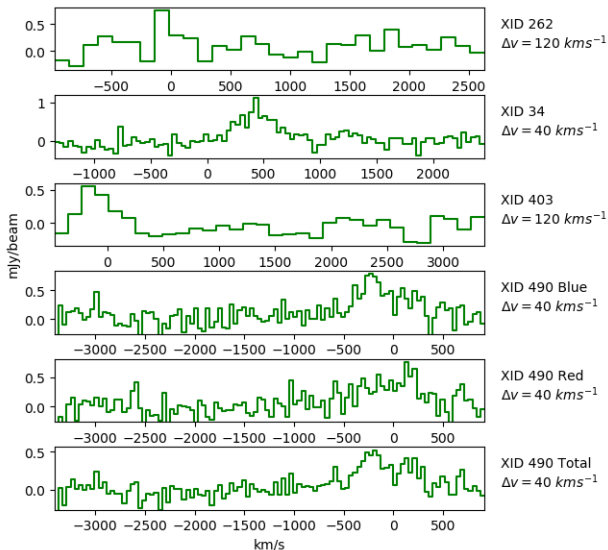
Outline

Scientific rationale and targets

Data analysis

Results

Conclusions and future perspectives



Dust mass

Outline

Scientific
rationale and
targets

Data analysis

Results

Conclusions
and future
perspectives

$$\begin{cases} L_\nu = \frac{4\pi D_L^2 S_{obs}}{1+z} \\ L_\nu = 4\pi j_\nu V \end{cases}$$

where z is the redshift, D_L is the luminosity distance, S_{obs} is the flux density at the observed frequency ν_{obs} , V is the volume of the source and j_ν is the specific emissivity per unit volume ($\text{erg s}^{-1} \text{ Hz}^{-1} \text{ ster}^{-1} \text{ cm}^{-3}$) that is equal to

$$j_\nu = \alpha_\nu B_\nu(T_d) = k_\nu \rho B_\nu(T_d)$$

$\alpha_\nu = k_\nu \rho$ is the opacity per unit of path length (cm^{-1}), k_ν is the opacity per mass unit ($\text{g}^{-1} \text{ cm}^2$) and $\rho = M_d/V$ is the density of the source (g cm^{-3}). M_d is the total mass of the dust.

The opacity per mass unit is assumed to scale with the frequency as $k_\nu = 4(\nu/1.2 \text{ THz})^\beta$ (draine+07). The index β is set equal to 2.0 (e.g., magnelli+12, gilli+14). Equalizing the two expressions of L_ν leads to the formula for the mass of the dust in the optically thin regime:

$$\frac{4\pi D_L^2 S_{obs}}{1+z} = 4\pi k_\nu \frac{M_d}{V} B_\nu(T_d) V$$

$$M_d = \frac{D_L^2 S_{obs}}{k_\nu B_\nu(T_d)(1+z)}$$

Interferometry

Outline

Scientific
rationale and
targets

Data analysis

Results

Conclusions
and future
perspectives

T_{SYS} : Temperature of a resistor emitting (as black body) a signal equal to the sum of all the contributions to the noise, placed above the atmosphere.

$$T_{SYS} = T_{atm}(e^{\tau} - 1) + T_{rx}e^{\tau}$$

T_{atm} : atmosphere, T_{rx} : instrument, τ : optical depth. Neglecting cosmic background (~ 3 K).

$$rms = \frac{2k_B T_{SYS}}{A_{eff} \sqrt{\Delta t \Delta \nu n_p N_{ant}(N_{ant} - 1)}}$$